

## **Natural Convection Heat Transfer in Rectangular Enclosure with Sinusoidal Boundary Condition**

*Ayad M. Salman*

*Assist Lecture*

*Energy and Fuel Research Center*

*University of Technology*

*Israa S. Ahmed*

*Assist Lecture*

*Electromechanical Eng. Dep*

*University of Technology*

*Sa'ib A. Hamid*

*Assist Lecture*

*Mech. Eng*

*Al-Mustansiriya University*

### **Abstract**

*Natural convection heat transfer with two-dimensional in a rectangular enclosure is examined numerically. The enclosure object with heated left side wall, while the right side was cold, the top and bottom walls was adiabatic. The theoretical study involved the numerical solution of the Navier-Stokes and energy equations by using finite difference method. The stream function– formulation was used in the mathematical model. The numerical solution is capable of calculating the velocity, stream function, and vorticity and temperature fields of the computational domain. A computer program in (FORTRAN 90) was used to carry out the numerical solution.*

*Problem has been analyzed and the non-dimensional governing equations are solved using finite difference method. Enclosure is assumed to be filled with an air with a Prandtl number of 0.71. The problem is analyzed for different values of the Rayleigh number in the range from  $10^3$  to  $10^5$ , aspect ratio parameter (AR: 1, 3, and 5). It is found that for small  $Ra$ , the heat transfer is dominated by conduction and begins to be dominated by convection with increasing  $Ra$ , and the Nusselt number  $Nu$  decreases with increasing AR due to decreasing the volume of the enclosure. In order to validate the numerical model, the results of variation local Nusselt number and a relation between average Nusselt number and  $Ra$  number, are compared with previous works. For square enclosure filled by air ( $Pr=0.72$ ). There are agreement in results and found excellent agreement which validate the present computational model.*

## انتقال الحرارة بالحمل الحر الانسيابي في حيز مغلق مستطيل مع شرط حدي موجي الشكل

## المستخلص

اجريت دراسة عددية لانتقال الحرارة بالحمل الحر في حيز مستطيل مغلق، الجدار العمودي في الجهة اليسرى يتعرض الى تسخين بينما الجدار العمودي في الجهة اليمنى يتعرض الى تبريد . وقد عزلت الاسطح العليا والسفلى من الحيز. الدراسة تضمنت الحل العددي لمعادلات نايفير-ستوك والطاقة باستخدام طريقة الفروقات المحددة. صيغة دالة الانسياب استخدمت في الموديل الرياضي. الحل العددي قادر على حساب السرعة، دالة الانسياب، الدوامية ودرجات الحرارة للمجال الحسابي. استخدم برنامج حاسوبي بلغة (FORTRAN 90) لحل المعادلات العددية. المسألة تم تحليلها والمعادلات اللابعدية الحاكمة تم حلها باستخدام طريقة الفروقات المحددة. الحيز مملوء بالهواء ويرقم براندل يساوي 0.72. رقم رايلي يتغير بمدى من  $10^3$  الى  $10^5$  ولنسبة باعية (AR: 1, 3, and 5). لقد وجد انه لقيم رايلي الصغيرة فإن انتقال الحرارة يكون بالتوصيل وانه يبدأ بالتحول الى الحمل مع ازدياد عدد رايلي ، وان عدد نسلت يقل مع زيادة النسبة الباعية . من اجل مصداقية الحل العددي، تم مقارنة النتائج التي الحصول عليها من العلاقة بين معدل عدد نسلت ورايلي مع بحث سابق، لحيز هوائي مربع الشكل ، (Pr=0.72)، وقد اوضحت النتائج تطابق جيد.

## Nomenclature

The following symbols are used generally throughout the text. Others are defined as and when used.

<u>Symbols</u>	<u>Meaning</u>
AR	Aspect ratio
$C_p$	Specific heat at constant pressure
$E_{max}$	Maximum error
g	Gravitational acceleration
H	Enclosure height
W	Enclosure Width
k	Thermal conductivity
Nu	Nusselt number
$\overline{Nu}$	Average Nusselt number
p	pressure
Pr	Prandtl number
Ra	Rayleigh number
$r, r_\psi, r_\Omega, r_\theta$	Relaxation parameter for stream function, vorticity, and temperature respectively
T	Temperature
u	Velocity component in x-direction
U	Dimensionless Velocity component in x-direction
v	Velocity component in y-direction
V	Dimensionless Velocity component in y-

	direction
x, y	Cartesian space coordinates
X,Y	Dimensionless Cartesian space coordinates

**Greek Symbol**

$\beta$	Coefficient of thermal expansion
$\phi$	General dependent variable
$\mu$	Molecular dynamic viscosity
$\nu$	Kinematic viscosity
$\omega$	Vorticity
$\Omega$	Dimensionless vorticity
$\rho$	Density of fluid
$\psi$	stream function
$\Psi$	Dimensionless stream function
$\theta$	Dimensionless temperature

**Subscript Symbols**

C, H	Related to cold and hot side respectively
(i,j)	Grid nodes in (x,y) direction

## 1.1 Introduction

Natural convection in a closed square cavity has occupied the center stage in many fundamental heat transfer analysis which is of prime importance in certain technological applications. In fact, buoyancy-driven convection in a sealed cavity with differentially heated isothermal walls is a prototype of many industrial applications such as energy efficient design of buildings and rooms, operation and safety of nuclear reactors and convective heat transfer associated with boilers. Buoyancy driven flows are complex because of essential coupling between the transport properties of flow and thermal fields.

## 1.2 Research Objective

Analyzing heat transfer within the fluid flow is important since it has many applications in industries such as energy conservation process, energy storage, meteorology and climatology. Numerical simulation plays an important role in these areas because experiments are often costly. The objectives of this research are listed below:

- i. Study the phenomena of natural convection inside a two-dimensional enclosure, which is differentially heated and cooled from the vertical walls.
- ii. Develop a program based on a finite difference method (FDM) and to validate the applied numerical method for the classical two-dimensional square cavity.

- iii. Investigate Determine the influence of Rayleigh number  $Ra$  on the velocity and temperature field inside a two-dimensional rectangular enclosure, which is heated and cooled from the vertical walls and adiabatic for top and lower walls.
- iv. Investigate the effect of aspect ratio on heat transfer and fluid flow inside a two-dimensional rectangular enclosure.
- v. The results will be in form of contours (stream function, and isotherm) and a plot between Nusselt number versus Rayleigh number will be done.
- vi. Comparisons with other investigations will be introduced to make sure from the present work results.

### **1.3 Literatures Survey**

Natural convection in rectangular enclosure has been studied for many years. In this item, the previous related literatures dealt with the subject of the research will be presented. Some of studies made a study on laminar natural convection in rectangular enclosure.

(M. Moghimi, H. Mirgolbabaei, Me. Miansari, Mo. Miansari, 2009) numerical study for steady laminar natural convection in air-filled, 2-D rectangular enclosures heated from below and cooled from above is for a wide variety of thermal boundary conditions at the sidewalls with effects of aspect ratio of the enclosure in the range between 0.25 and 1, and the Rayleigh number based on the cavity height in the range between  $1.00e3$  and  $5.00e5$ . (G. Gediz Ilis, M. Mobedi, B. Sunden , 2008) numerically investigated for entropy generation in rectangular cavities with the same area but different aspect ratios. The vertical walls of the cavities are at different constant temperatures while the horizontal walls are adiabatic. Heat transfer between vertical walls occurs by laminar natural convection. The study is performed for range of Rayleigh number  $Ra$   $10^2$  to  $10^5$  and  $Pr=0.7$ . (T. Basak, S. Roy, A.R. Balakrishnan ,2006) investigate numerical study to the steady laminar natural convection flow in a square cavity with uniformly and non-uniformly heated bottom wall, and adiabatic top wall maintaining constant temperature of cold vertical walls has been performed. The study yields consistent performance over a wide range of parameters (Rayleigh number  $Ra$ ,  $10^3$  to  $10^5$  and Prandtl number  $Pr$ , 0.7 to 10. (O. Zeitoun and Mohamed Ali, 2006) studied numerically two-dimensional laminar natural-convection heat transfer in air around horizontal ducts with rectangular and square cross sections. Different aspect ratios are used for wide ranges of Rayleigh numbers. (I. E. Sarris, I. Lekakis, and N. S. Vlachos, 2002) investigated numerically natural convection in a two-dimensional, rectangular enclosure with sinusoidal temperature profiles on the upper wall and adiabatic conditions on the bottom and sidewalls . The applied sinusoidal temperature is symmetric with respect to the midplane of the enclosure. Numerical calculations are produced for Rayleigh numbers in the range  $10^2$  to  $10^8$ .

In this study, natural convection in enclosure with non-uniform heating from the left side wall and cold with uniform temperature on the right side wall and adiabatic on the top and bottom. The effect of Rayleigh number on the flow patterns and the resulting heat transfer is determined. In addition the effect of the enclosure aspect ratio is studied for the value of Rayleigh numbers from  $10^3$  to  $10^5$ .

The numerical technique based on the finite difference method (FDM) is generally applied in the computations of a uniform grid size. The results are presented in tabular form of the average Nusselt number,  $\overline{Nu}$ , which represents the rate of heat being transferred. In addition, the results are also presented in graphical forms of stream function and isotherms contours, which demonstrate the fluid flow and thermal distributions inside the enclosure.

## 2.1 Mathematical Model

In this research, first give the basic equations of the mass and momentum conservations (Navier-Stokes equations) in terms of primitive variables for an incompressible, viscous fluid. This formulation contains the velocity and the pressure of the fluid which are the original unknowns. The difficulties arise due to the satisfaction of the continuity equation and missing pressure equation. Thus, in most of the numerical procedures these equations are transformed to stream function-vorticity and velocity-vorticity formulations. A schematic diagram of the physical situation is presented in Fig. 1. In this item, the main equations for the laminar natural convection through two-dimensional enclosure with appropriate boundary conditions.

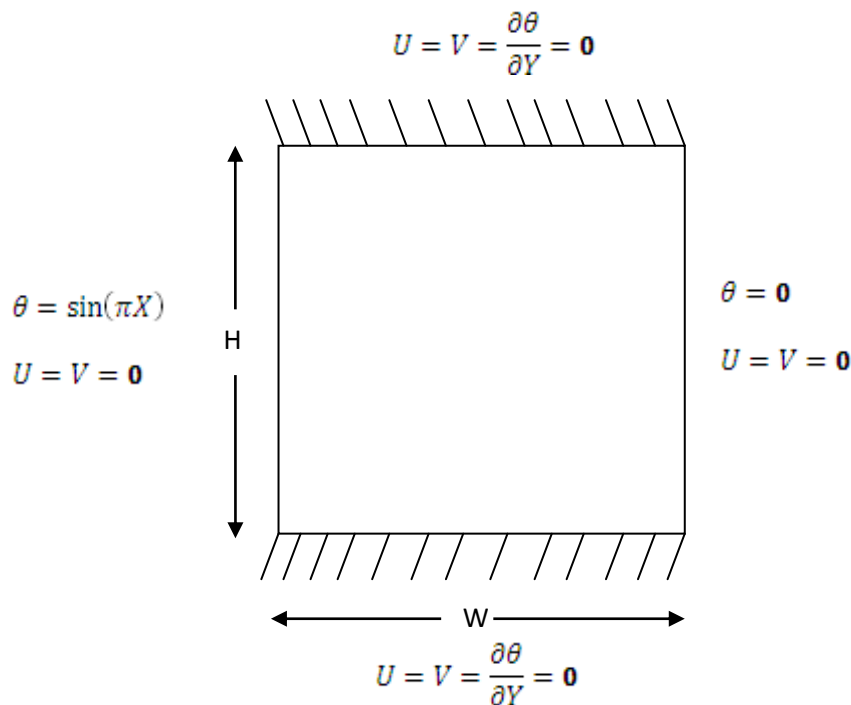


**Fig.1. Schematic diagram of the physical configuration and boundary**

Following assumptions have been made: two-dimensional problem, there is no viscous dissipation, the gravity acts in the vertical direction, the fluid properties are constant and radiation heat exchange was assumed negligible. At steady state conditions using above assumption, the governing equations as given below (Diaz and Winston, 2008):

**Continuity equation:**

$$\frac{\partial u}{\partial x} + \frac{\partial v}{\partial y} = 0 \quad (1)$$

**x-momentum equation:**

$$u \frac{\partial u}{\partial x} + v \frac{\partial u}{\partial y} = -\frac{\partial p}{\partial x} + \nu \left( \frac{\partial^2 u}{\partial x^2} + \frac{\partial^2 u}{\partial y^2} \right) \quad (2)$$

**y-momentum equation:**

$$u \frac{\partial v}{\partial x} + v \frac{\partial v}{\partial y} = -\frac{\partial p}{\partial y} + \nu \left( \frac{\partial^2 v}{\partial x^2} + \frac{\partial^2 v}{\partial y^2} \right) + g\beta(T - T_c) \quad (3)$$

**Energy equation**

$$u \frac{\partial T}{\partial x} + v \frac{\partial T}{\partial y} = \frac{\nu}{Pr} \left( \frac{\partial^2 T}{\partial x^2} + \frac{\partial^2 T}{\partial y^2} \right) \quad (4)$$

The governing equations are transformed into dimensionless forms under the following non-dimensional variables (T. Basak, S. Roy, A.R. Balakrishnan ,2006):

$$U = \frac{uH}{g} = \frac{\partial \Psi}{\partial Y}, Y = \frac{y}{H} \quad (5)$$

$$U = \frac{vH}{g} = -\frac{\partial \Psi}{\partial X}, X = \frac{x}{H} \quad (6)$$

$$\theta = \frac{T - T_c}{T_h - T_c}, Gr = \frac{g\beta W^3 (T_h - T_c)}{g^2}; Pr = \frac{\mu C_p}{k}; Ra = GrPr \quad (7)$$

In terms of these variables, the stream function, vorticity and energy equations respectively becomes

$$\left(\frac{\partial^2\Psi}{\partial X^2} + \frac{\partial^2\Psi}{\partial Y^2}\right) = -\Omega \tag{8}$$

$$\frac{\partial\Psi}{\partial Y} \frac{\partial\Omega}{\partial X} - \frac{\partial\Psi}{\partial X} \frac{\partial\Omega}{\partial Y} = \text{Pr}\left(\frac{\partial^2\Omega}{\partial X^2} + \frac{\partial^2\Omega}{\partial Y^2}\right) - Ra \frac{\partial\theta}{\partial X} \tag{9}$$

$$\frac{\partial\Psi}{\partial Y} \frac{\partial\theta}{\partial X} - \frac{\partial\Psi}{\partial X} \frac{\partial\theta}{\partial Y} = \left(\frac{\partial^2\theta}{\partial X^2} + \frac{\partial^2\theta}{\partial Y^2}\right) \tag{10}$$

## 2.2 Boundary Conditions

The boundary conditions of velocity and temperature fields are shown in Fig .1 presented as (Oosthuizen and Naylor, 1999):

$$\left. \begin{aligned} X = 0: u = v = \Psi = 0, \theta = \text{Sin}(\pi X), -\Omega = \frac{\partial^2\Psi}{\partial X^2} \\ X = 1: u = v = \Psi = 0, \theta = 0, -\Omega = \frac{\partial^2\Psi}{\partial X^2} \\ Y = 0: u = v = \Psi = 0, \frac{\partial\theta}{\partial Y} = 0, -\Omega = \frac{\partial^2\Psi}{\partial Y^2} \\ Y = 1: Y = 0: u = v = \Psi = 0, \frac{\partial\theta}{\partial Y} = 0, -\Omega = \frac{\partial^2\Psi}{\partial Y^2} \end{aligned} \right\} \tag{11}$$

The rate of heat transfer is expressed in terms of local Nusselt number, Nu, at the heated section as follows:

$$Nu = -\frac{\partial\theta}{\partial X}\bigg|_{X=0} \quad ; \quad 0 \leq Y \leq 1 \tag{12}$$

The average Nusselt number,  $\overline{Nu}_h$ , is defined by:

$$\overline{Nu} = \frac{1}{L} \int_0^L Nu dY \tag{13}$$

### 3.1 Numerical Solution

The method of numerical solution taken is the central finite difference scheme technique for convert the partial differential equation to an algebraic which can be solved numerically. The energy equation is a nonlinear partial differential equation, which has (convection terms) on the left hand side of the eq. 10 and (diffusion term) on the right hand side. To convert the convection and diffusion terms to algebraic terms, central difference scheme will be used, as below (Tannehill et al.

$$(1997)) \left( \frac{\Psi_{i,j+1} - \Psi_{i,j-1}}{2\Delta Y} \right) \left( \frac{\theta_{i+1,j} - \theta_{i-1,j}}{2\Delta X} \right) - \left( \frac{\Psi_{i+1,j} - \Psi_{i-1,j}}{2\Delta X} \right) \left( \frac{\theta_{i,j+1} - \theta_{i,j-1}}{2\Delta Y} \right) = \left( \frac{\theta_{i+1,j} - 2\theta_{i,j} + \theta_{i-1,j}}{\Delta X^2} \right) + \left( \frac{\theta_{i,j+1} - 2\theta_{i,j} + \theta_{i,j-1}}{\Delta Y^2} \right) \quad (14)$$

This can be rearranged to give:

$$\theta_{i,j} = \left\{ \left( \frac{-1}{4\Delta X \Delta Y} \right) \left[ (\Psi_{i,j+1} - \Psi_{i,j-1})(\theta_{i+1,j} - \theta_{i-1,j}) - (\Psi_{i+1,j} - \Psi_{i-1,j})(\theta_{i,j+1} - \theta_{i,j-1}) \right] + \left( \frac{\theta_{i+1,j} + \theta_{i-1,j}}{\Delta X^2} + \frac{\theta_{i,j+1} + \theta_{i,j-1}}{\Delta Y^2} \right) \right\} / \left( \frac{2}{\Delta X^2} + \frac{2}{\Delta Y^2} \right) \quad (15)$$

Similarity, the finite difference form of the vorticity transport equation, i.e., eq. 9, gives:

$$\left( \frac{\Psi_{i,j+1} - \Psi_{i,j-1}}{2\Delta Y} \right) \left( \frac{\Omega_{i+1,j} - \Omega_{i-1,j}}{2\Delta X} \right) - \left( \frac{\Psi_{i+1,j} - \Psi_{i-1,j}}{2\Delta X} \right) \left( \frac{\Omega_{i,j+1} - \Omega_{i,j-1}}{2\Delta Y} \right) = \left[ \left( \frac{\Omega_{i+1,j} - 2\Omega_{i,j} + \Omega_{i-1,j}}{\Delta X^2} \right) + \left( \frac{\Omega_{i,j+1} - 2\Omega_{i,j} + \Omega_{i,j-1}}{\Delta Y^2} \right) \right] + Gr \left( \frac{\theta_{i+1,j} - \theta_{i-1,j}}{2\Delta X} \right) \quad (16)$$

This can be rearranged to give:

$$\Omega_{i,j} = \left\{ \left( \frac{-1}{4\Delta X \Delta Y Pr} \right) \left[ (\Psi_{i,j+1} - \Psi_{i,j-1})(\Omega_{i+1,j} - \Omega_{i-1,j}) - (\Psi_{i+1,j} - \Psi_{i-1,j})(\Omega_{i,j+1} - \Omega_{i,j-1}) \right] + \left( \frac{\Omega_{i+1,j} + \Omega_{i-1,j}}{\Delta X^2} + \frac{\Omega_{i,j+1} + \Omega_{i,j-1}}{\Delta Y^2} \right) + Ra \left( \frac{\theta_{i+1,j} - \theta_{i-1,j}}{2\Delta X} \right) \right\} / \left( \frac{2}{\Delta X^2} + \frac{2}{\Delta Y^2} \right) \quad (17)$$

Lastly,

the finite difference form of the equation relating the dimensionless stream function, i.e., eq. 8, is:

$$\Psi_{i,j} = \left[ \left( \frac{\Psi_{i+1,j} + \Psi_{i-1,j}}{\Delta X^2} + \frac{\Psi_{i,j+1} + \Psi_{i,j-1}}{\Delta Y^2} \right) + \Omega_{i,j} \right] / \left( \frac{2}{\Delta X^2} + \frac{2}{\Delta Y^2} \right) \quad (18)$$

### 3.2 Solution Procedure

The governing dimensionless differential equations are discretized to a finite difference form is used. The computational scheme, based on Successive Over Relaxation, SOR, is arranged to solve the three equations for the nth iteration step. The initial values over the field for  $\theta$ ,  $\omega$  and  $\psi$  are assumed zero to all internal nodes are taken as initial starting values. Over-relaxation is actually used so the "updated" values of  $\phi_{i,j}$  are actually taken as:

$$\phi_{i,j}^{new} = \phi_{i,j}^{old} + r(\phi_{i,j}^{calculated} - \phi_{i,j}^{old}) \quad (19)$$

Where the subscripts i and j refer to a grid node,  $\phi$  is a general dependent variable ( $\theta$ ,  $\omega$ , or  $\psi$ ). The relaxation parameters,  $\gamma_\theta = \gamma_\omega = 1$  and  $\gamma_\psi = 1.6$  give stable numerical computation  $Ra \leq 10^4$ .

The criterion for convergence is examined according to a realistic condition for each state variable at each node as:

$$\frac{|\phi_{i,j}^{new} - \phi_{i,j}^{old}|}{|\phi_{i,j}^{old}|} \leq E_{max} \quad (20)$$

Where the subscripts i and j refer to a grid node,  $\phi$  is a general dependent variable ( $\theta$ ,  $\omega$ , or  $\psi$ ) and  $E_{max}$  is a small quantity of error set to  $10^{-5}$  for  $Ra \leq 10^5$ .

A computer program in (Fortran 90) was built to execute the numerical algorithm which is mentioned above; it is general for a natural convection in two-dimensional annular enclosure.

## 5. Result and Discussions:

### 5.1 Numerical Results Verification

In order to validate the numerical model, the results of variation local Nusselt number and a relation between average Nusselt number and Ra number, are compared with previous works. For square enclosure filled by air (Pr=0.72) the results are compared with (Lo et al. 2007).

There are agreement in results and found excellent agreement which validate the present computational model as shown in Figs (2) and (3).

Numerical simulations are performed for  $Pr = 0.72$  (air is the working fluid) and different values of both the Rayleigh number in the range  $103 \leq Ra \leq 105$ , the aspect ratio of the cavity in  $1 \leq AR \leq 5$ , in order to point out the influence of  $Ra$  and  $AR$  upon the flow structure type and the temperature distributions throughout the cavity, sample local results are reported in terms of isotherms and streamlines. In all the isotherm plots, the contour lines correspond to equispaced values of the dimensionless temperature  $\theta$  in the range between 0 and 1. In all the streamline plots, the contour lines correspond to equispaced absolute values of the normalized dimensionless stream function in the range between 0 and 1. The temperature distribution and the flow field due to buoyancy-forces in a rectangular enclosure filled with air with the temperature distribution of the left wall varying sinusoidally has been analyzed numerically for different values of the aspect ratio  $AR$ , Rayleigh number  $Ra$ .

## **5.2 Isotherms and Streamlines**

Results for isotherms, streamlines and vorticity are presented with effect of Rayleigh number ( $Ra=103, 104, 105$ ) and  $AR=1.0$  are shown in fig.(4) to show the effect of the Rayleigh number  $Ra$  on the free convection flow. It is seen that the streamline contours exhibit circulation patterns, which are characterized by the three vortices. The fluid motion, as it is driven by the effect of the buoyancy, is distributed from the heated part of the right side wall through the inside of the enclosure. Two small cells were formed in the upper and bottom corners in clockwise and counterclockwise rotating direction, respectively. However, a huge main cell was formed with its center located almost in the middle of the enclosure, as shown in Fig.4 (b). The center of the cell moves towards the right upper corner with increasing of  $Ra$  (Fig.4 (b)). The range of Rayleigh numbers 103 to 104, the circulation patterns in the enclosure are very weak because the viscous forces are dominating over the buoyant forces. The flow strength increases with increasing of  $Ra$  and it can be seen from the values of the stream function on the streamline. The length and locations of the small cells become almost the same when the values of the Rayleigh number are changed. Isotherms show an almost symmetrical distribution for low Rayleigh number due to domination of conduction mode of heat transfer. It can be seen from the isotherm contours the temperature fronts penetrate from the right side wall deep inside the fluid body, as conduction is the main heat transfer mechanism in this case. With increasing Rayleigh number, at approximately  $Ra = 105$ , the isotherms start to concentrate near the right side wall, indicating that the advection mode of the heat transfer begins to dominate over conduction.

Figs (5,6) shows the flow field and temperature distribution at different values of ( $AR=3,5$ ) respectively when ( $Ra=103,104,105$ ), it can be seen that with increasing aspect ratio, number

of vorticity will be increased. For instance, when ( $AR=3$ ), we see three vorticities, and when ( $AR=5$ ), we see five vorticities which are circulating in the opposite directions. It can be seen that with increasing aspect ratio, there are more possibility of appearance of more columns of cold and hot air which causes more vorticity.

### 5.3 Temperature and velocity distribution

The temperature distribution in the middle plane of the enclosure, shown in Fig.(8), is quite helpful in assessing the penetration depth of the temperature boundary layer formed on the right wall of the enclosure. In particular, for every Rayleigh number studied, the dimensionless temperature takes the value of 1 at the right of the middle plane of the enclosure and then decreases with increasing distances from the right wall. Conduction and convection are the two antagonistic mechanisms depending on the specific value of Rayleigh number. In the case of the lower Rayleigh number of 103, the middle-plane temperature  $Y_{mp}$  reaches an asymptotic value in the core region of the enclosure that corresponds to the heat transfer by pure conduction. The increase in the  $Ra$  number causes a decrease in the asymptotic value of the middle-plane temperature in the core region, as a consequence of the dominance of convective heat transfer. In this last case, the thermal boundary layer becomes thinner, indicating that the heat transfer takes place in the region near the right wall without much penetration into the main fluid body.

Fig.(9) show the relation between the component velocity( $u$ ) with the dimensionless distance ( $Y$ ) in the middle plane of the enclosure, with effect of aspect ratio ( $AR=1,3,5$ ), it can see that this component take sine wave shape and this waving increase with increase the aspect ratio, on other hand the  $u$ -component magnitude increase with increase Rayleigh number ( $Ra$ ).

Fig.(10) show the relation between the component velocity( $v$ ) with the dimensionless distance ( $X$ ) in the middle plane of the enclosure, with effect of aspect ratio ( $AR=1,3,5$ ), it can see that this component variation from positive to negative value and take a (0) value at ( $X=0$ ), and its magnitude increase with increase the aspect ratio, on other hand the  $v$ -component magnitude increase with increase Rayleigh number ( $Ra$ ).

### 5.4 The Variation of Nusselt Number

Results of the local Nusselt number  $Nu$  are presented in Fig. 7 (a) to (c), shows the effect of  $Ra$  on the variation of the local Nusselt number with the coordinate  $Y$ . It is seen that  $Nu$  is positive when the heat is transferred into the enclosure and negative when it is transferred from the enclosure to the environment. The maximum value of  $Nu$  increases with increasing the Rayleigh number in both positive and negative regions due to the increase of the effect of convection mode of heat transfer, and we can obtain the effect of  $AR$  on  $Nu$ , the effect of  $AR$

is very small, but  $Nu$  decreases with increasing  $AR$  due to decreasing the volume of the enclosure. However  $AR$  shows small variation of  $Nu$ . On the contrary,  $Nu$  increases with decreasing of  $AR$  due to low volume of the enclosure.

## **6. Conclusions**

In this research natural convection in (air,  $Pr=0.72$ ) filled rectangular enclosure, the enclosure consist of top and bottom adiabatic surfaces, two isotherm vertical walls, non-uniform temperature distribution on the hot right wall, uniform temperature distribution on the cold right wall. The partial differential equations for two dimensional in stream-vorticity form and energy equation are solved based on central finite difference scheme. The solution scheme is validated by comparison with last research, where the agreement was excellent, and we can take the following conclusions that found from the results of the present work:

- 1- For small  $Ra$ , the heat transfer is dominated by conduction across the fluid layers, and the process begins to be dominated by convection with increasing  $Ra$ .
- 2- When the  $AR=1$ , there are appear main cell with two eddy cell, but when increasing aspect ratio, number of vorticity will be increased. For instance, when ( $AR=3$ ), we see three vorticities, and when ( $AR=5$ ), we see five vorticities which are circulating in the opposite directions.
- 3- The local Nusselt number  $Nu$  is positive when the heat is transferred into the enclosure and negative when it is transferred from the enclosure.
- 4- The maximum value of  $Nu$  increases with increasing the Rayleigh number in both positive and negative regions due to the increase of the effect of convection mode of heat transfer.
- 5- Nusselt number  $Nu$  decreases with increasing  $AR$  due to decreasing the volume of the enclosure.

## References

1. M. Moghimi, H. Mirgolbabaei, Me. Miansari, Mo. Miansari, “**Natural Convection in Rectangular Enclosures Heated From Below and Cooled from Above**”, *Australian Journal of Basic and Applied Sciences*, 3(4): 4618-4623, 2009.
2. Gamze Gediz Ilis, Moghtada Mobedi, Bengt Sunden, “**Effect of aspect ratio on entropy generation in a rectangular cavity with differentially heated vertical walls**”, *International Communications in Heat and Mass Transfer* 35, 696–703, (2008).
3. Tanmay Basak , S. Roy , A.R. Balakrishnan “**Effects of Thermal Boundary Conditions on Natural Convection Flows within a Square Cavity**” , *International Journal of Heat and Mass Transfer* 49, 4525–4535 , 2006.
4. O. Zeitoun and Mohamed Ali, “**Numerical Investigation of Natural Convection Around Isothermal Horizontal Rectangular Ducts**”, *Numerical Heat Transfer, Part A*, 50: 189–204, 2006.
5. I. E. Sarris, I. Lekakis, and N. S. Vlachos “**Natural Convection in a 2D Enclosure with Sinusoidal Upper Wall Temperature**”, *Numerical Heat Transfer, Part A*, 42: 513-530, 2002.
6. Diaz, Gerardo and Winston, Roland, "**Effect of Surface Radiation on Natural Convection in Parabolic Enclosures**", *J. Numerical Heat Transfer, Part A*, Vol. 53, pp.(891–906), 2008.
7. Oosthuizen, Patirick H. and Naylor, David, "**An Introduction to Convective Heat Transfer Analysis**", *International Edition, WCB/McGraw Hill, New York*, (1999).
8. Tannehill, John C., Anderson, Dale A., Pletcher, Richard H., "**Computation fluid mechanics and heat transfer**", *2nd Edition, Taylor & Francis, USA*, 1997.
9. Lo, D.C., Young, D.L. and Tsai, C.C., "**High resolution of 2D natural convection in a cavity by the DQ method**", *J. Computational and Applied Mathematics*, Vol. 203, pp. (219 – 236), 2007.

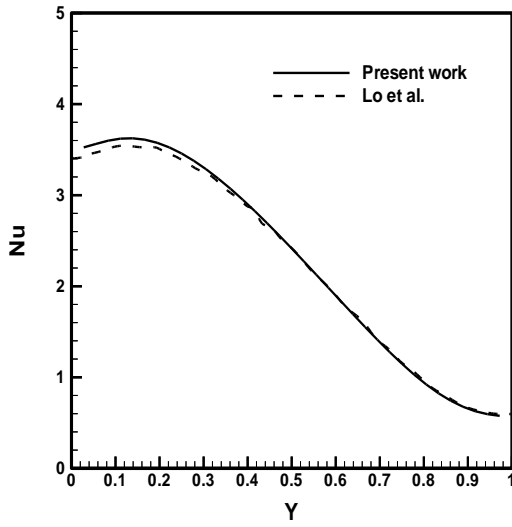


**Fig ( 2 ):** show comparison between present

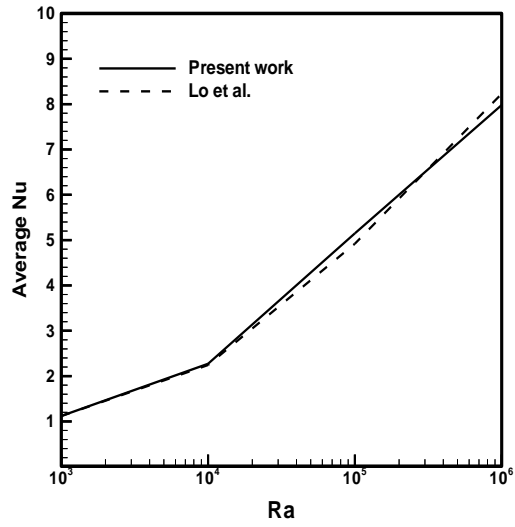


**Fig ( 3 ):** show comparison between present work and Lo et al. for relation between  $Nu$  and  $Ra$ .

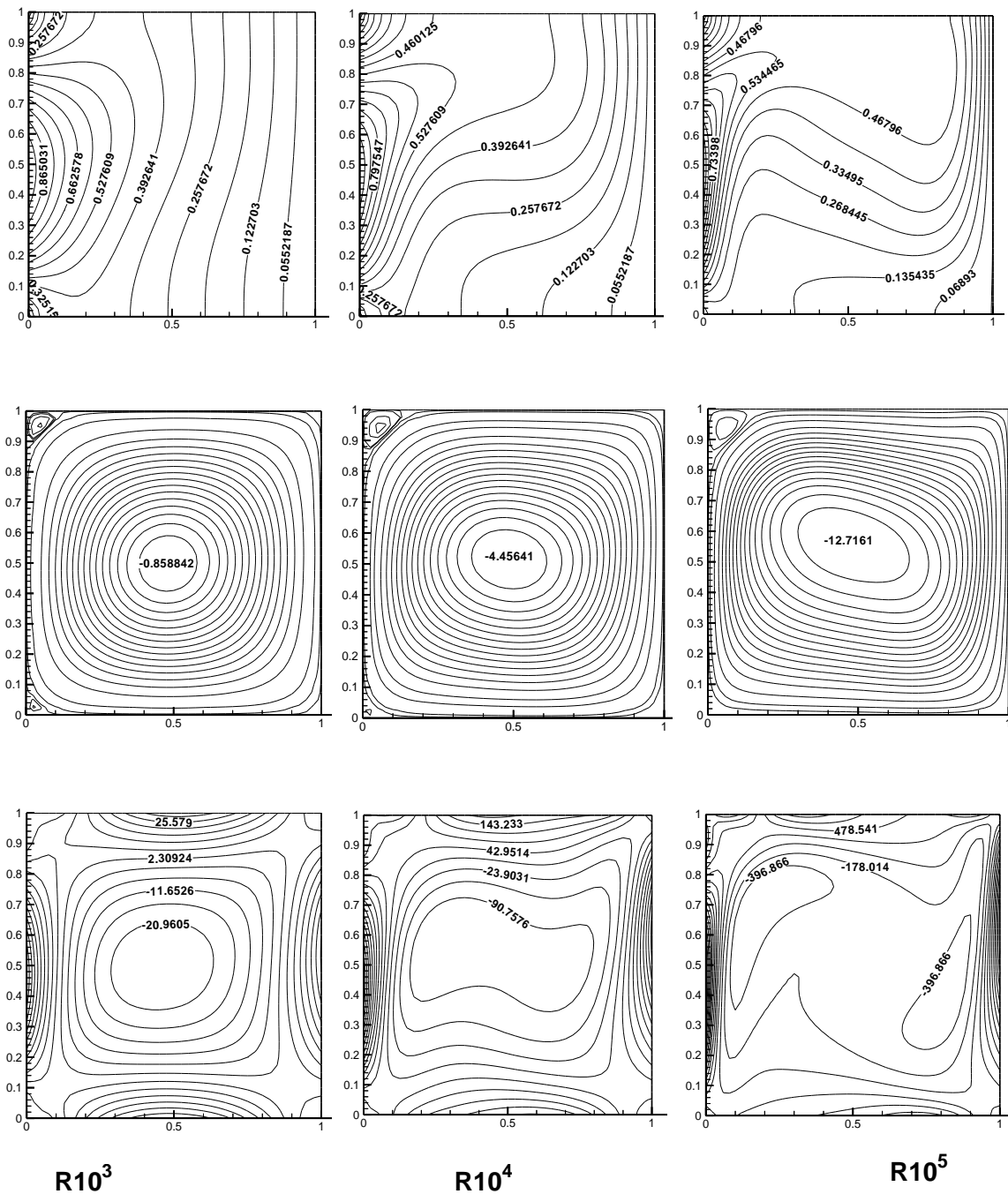


**Fig4. Isotherms; streamlines and vorticity contours of non-uniform heated left wall, uniform cold right wall and adiabatic top and bottom walls inside rectangular enclosure with aspect ratio (AR=1).**

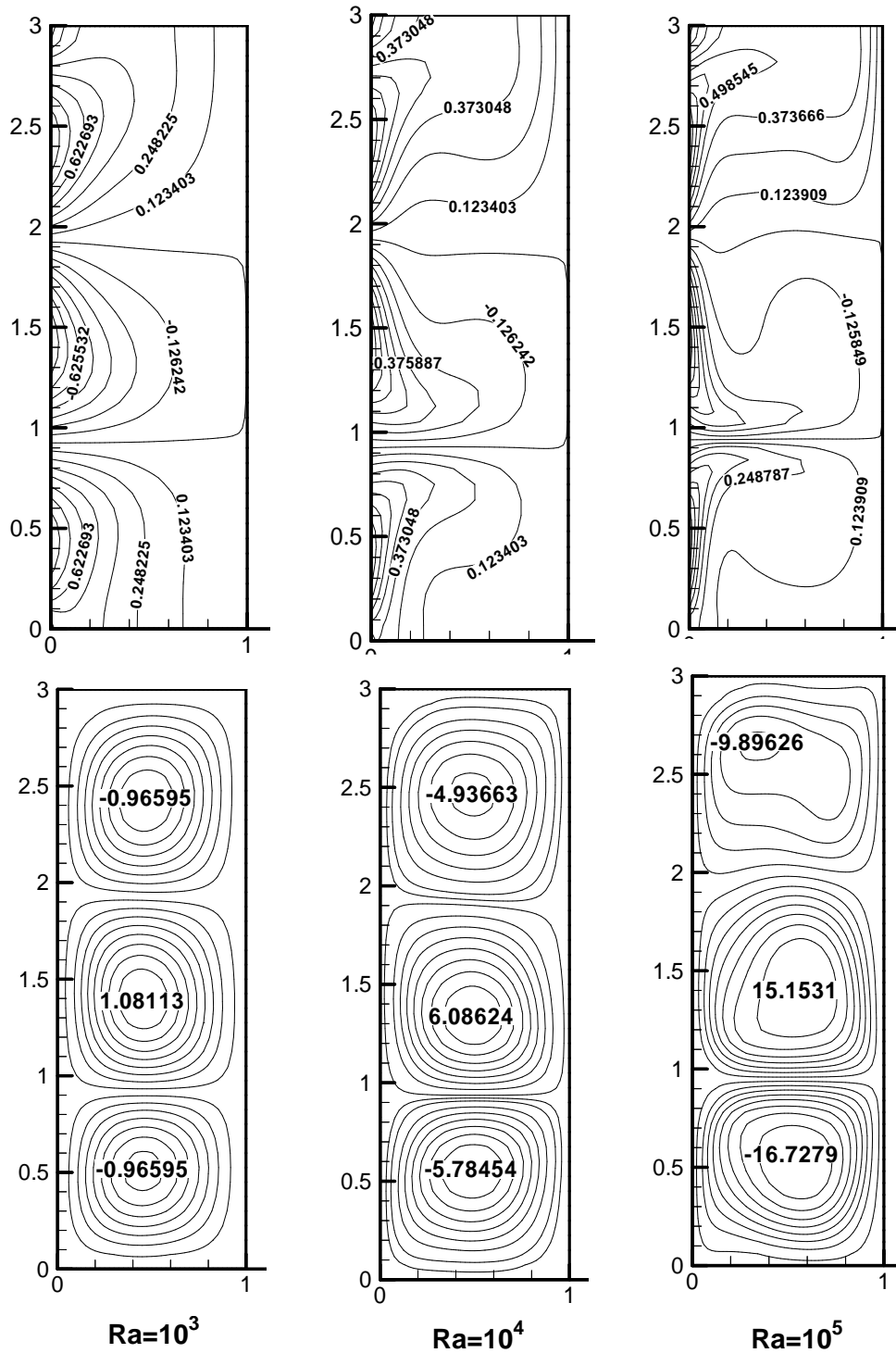


**Fig5. Isotherms and streamlines contours of non-uniform heated left wall, uniform cold right wall and adiabatic top and bottom walls inside rectangular enclosure with aspect ratio (AR=3).**

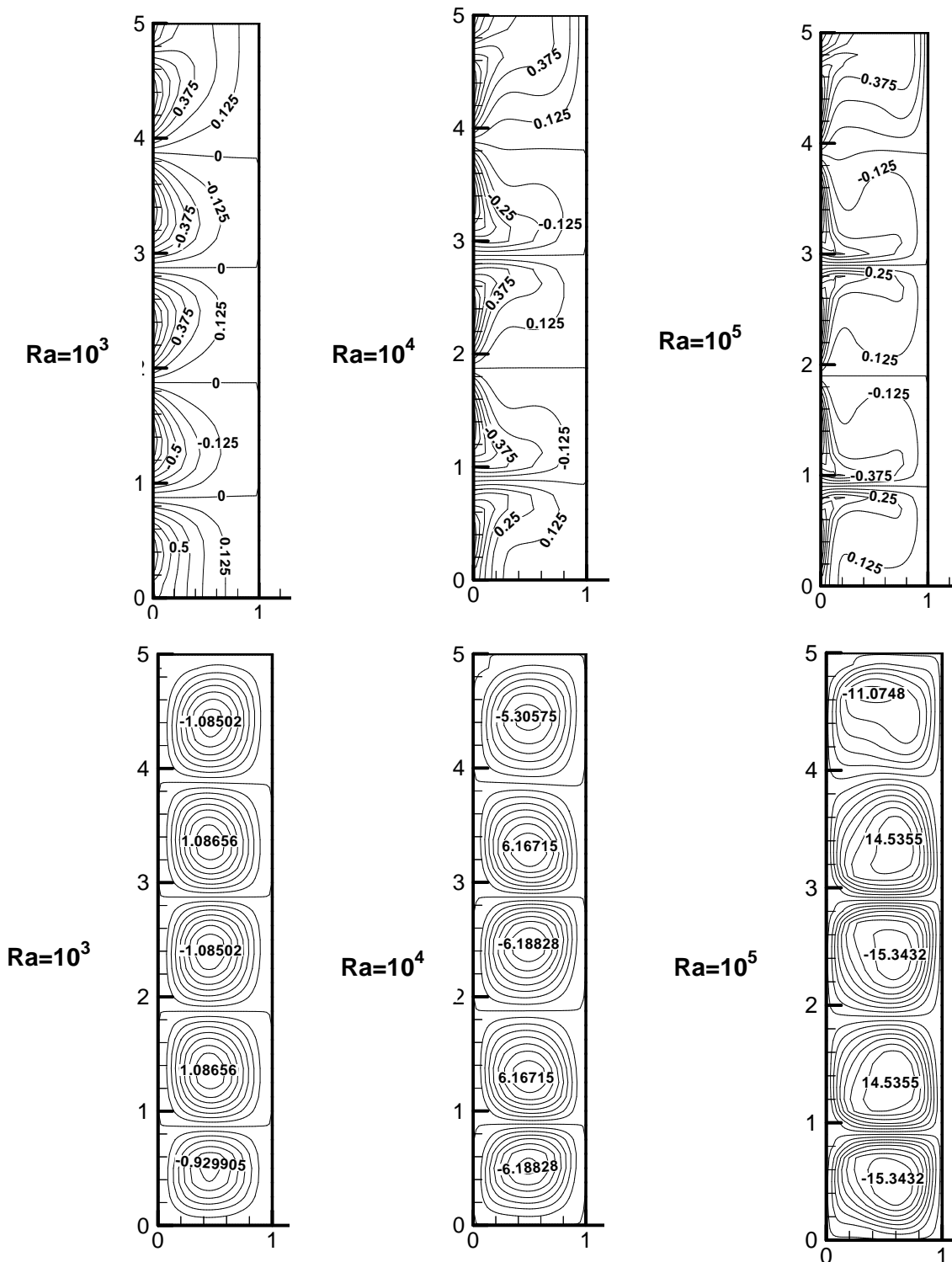


**Fig6. Isotherms and streamlines contours of non-uniform heated left wall, uniform cold right wall and adiabatic top and bottom walls inside rectangular enclosure with aspect ratio (AR=5).**

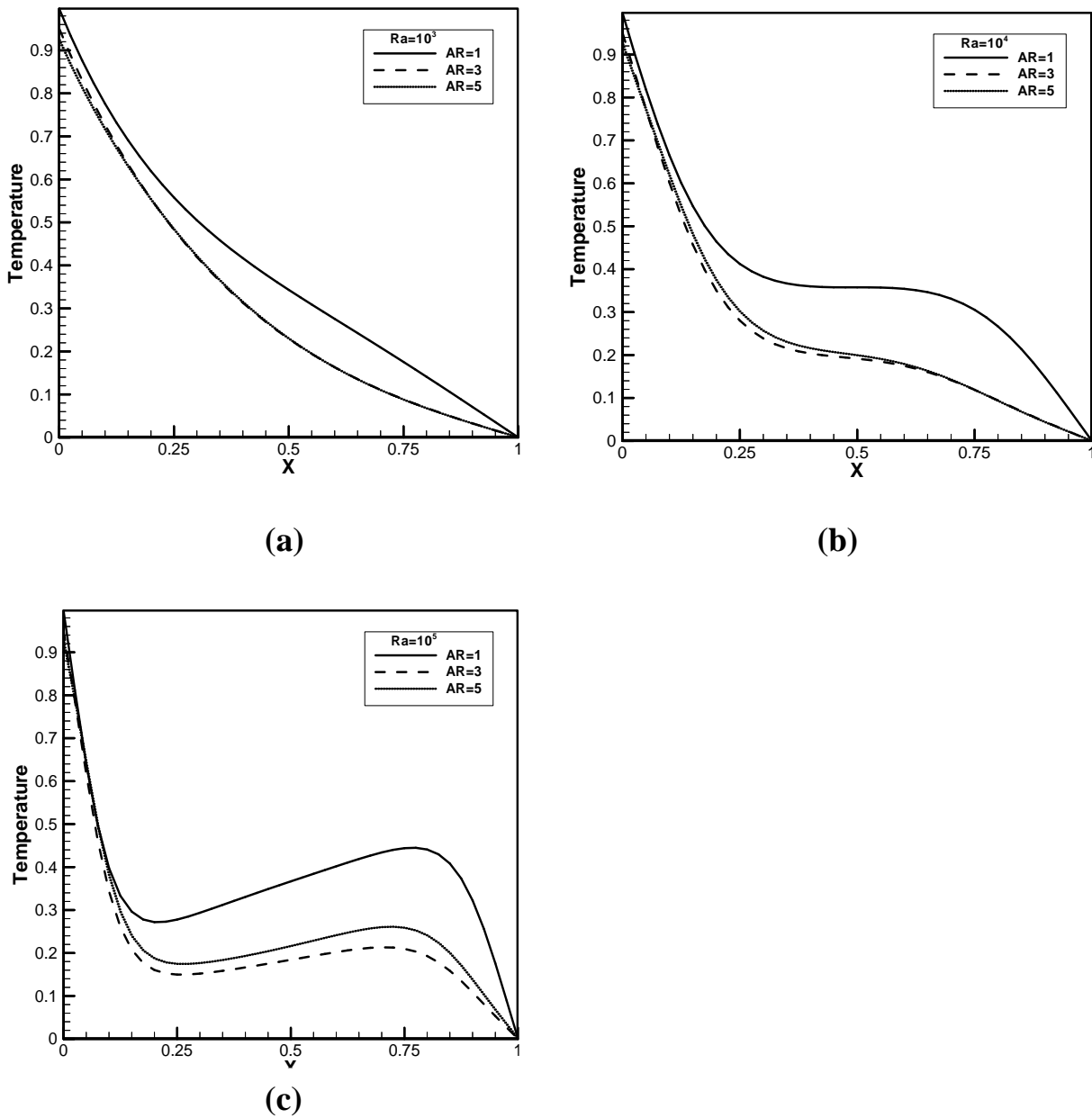
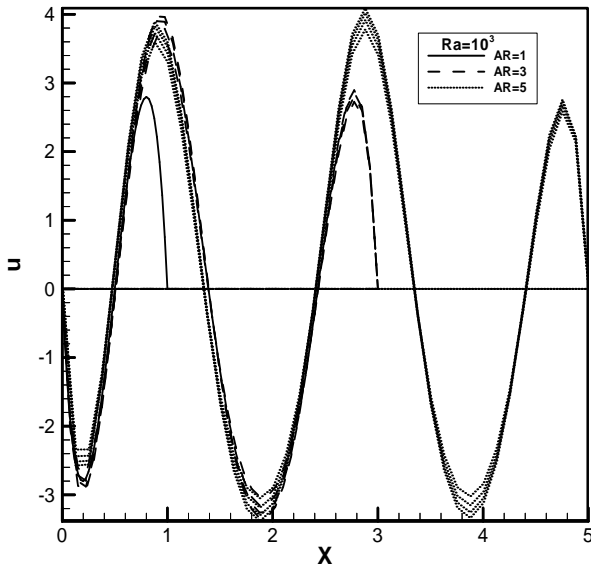
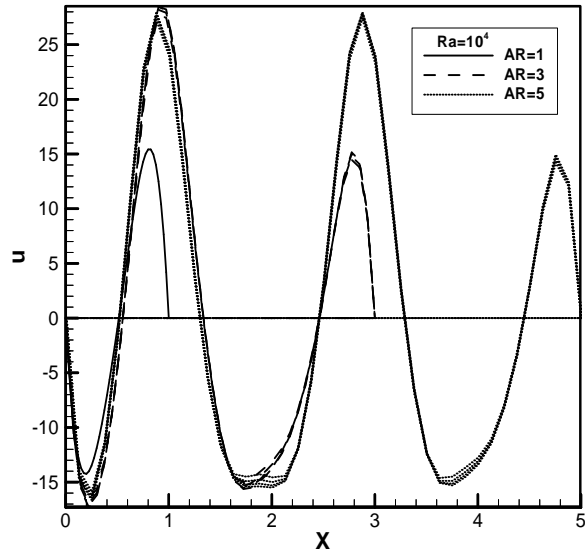


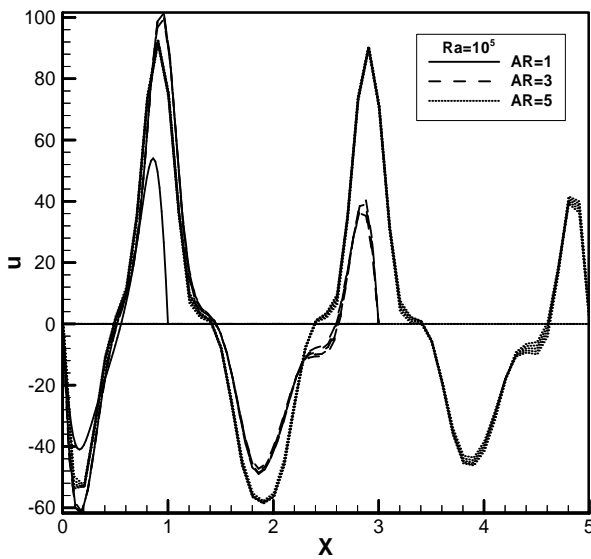
**Fig. (8) Temperature distribution on the dimensionless distance  $Y$  with effect of aspect ratio ( $AR=1, 3, 5$ ); (a)  $Ra=10^3$ , (b)  $Ra=10^4$ , (c)  $Ra=10^5$ .**



(a)

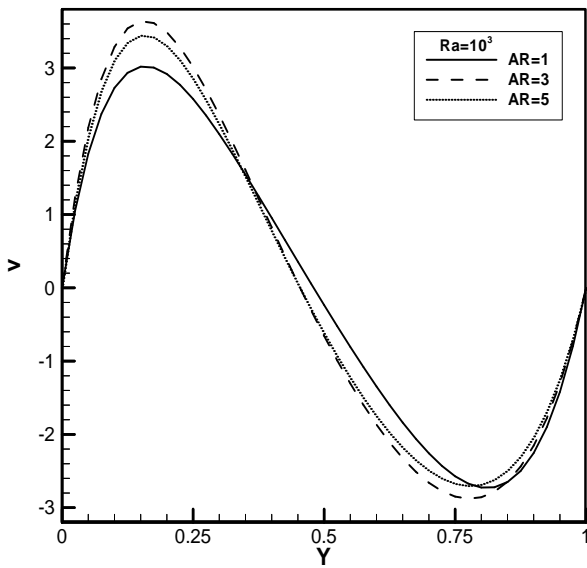


(b)

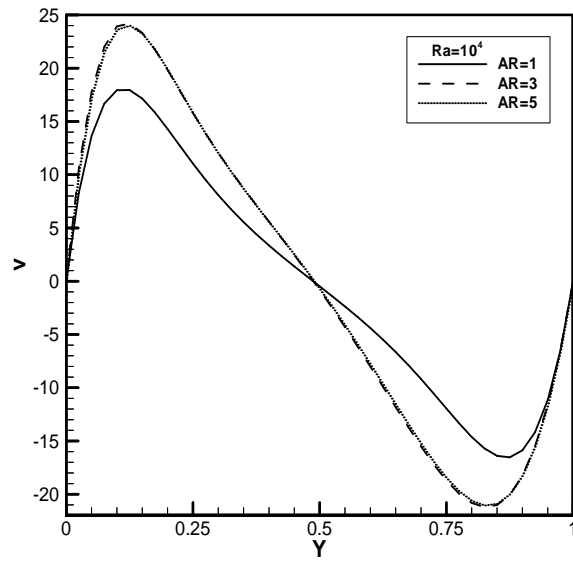


(c)

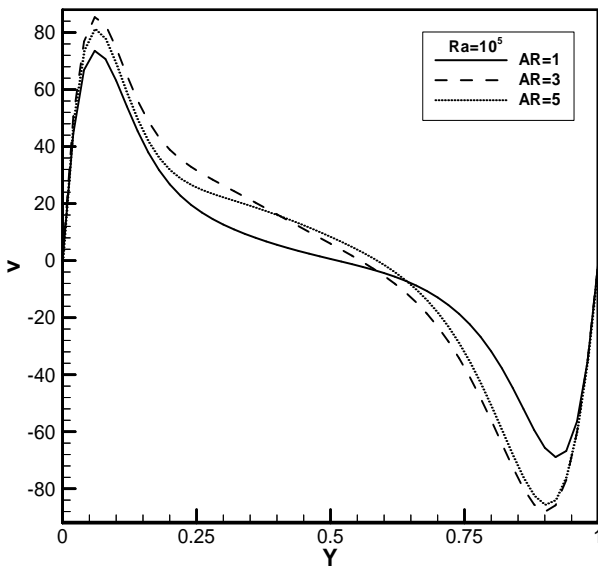
**Fig. (9) Velocity distribution ( $u$ ) on the dimensionless distance  $Y$  with effect of aspect ratio ( $AR=1, 3, 5$ ); (a)  $Ra=10^3$ , (b)  $Ra=10^4$ , (c)  $Ra=10^5$ .**



(a)



(b)



(c)

**Fig. (10) Velocity distribution ( $v$ ) on the dimensionless distance  $X$  with effect of aspect ratio ( $AR=1, 3, 5$ ); (a)  $Ra=10^3$ , (b)  $Ra=10^4$ , (c)  $Ra=10^5$ .**